Molecular weight effects on phase transitions of side-chain liquid crystalline poly(vinyl ether)s with terminal alkoxybiphenyl groups

Toshihiro Sagane* and Robert W. Lenz†
Polymer Science and Engineering Department, University of Massachusetts, Amherst, MA 01003, USA
(Received 23 January 1989; accepted 16 February 1989)

Two vinyl ether monomers with alkoxybiphenyl groups, 2-(4′-ethoxy-4-biphenyloxy)ethyl vinyl ether (EtOVE) and 2-(4′-hexyloxy-4-biphenyloxy)ethyl vinyl ether (HexOVE), were polymerized by living cationic polymerization reactions using either the hydrogen iodide/iodine (HI/I_2) or the hydrogen iodide/zinc iodide (HI/ZnI_2) initiator systems, or both. These initiators yield polymers with narrow molecular weight distributions (MWDs) and for comparison broad MWD polymers were also prepared by using the BF_3OEt_2 initiator. The thermal properties and phase transitions of these polymers were determined by differential scanning calorimetry, by visual observations of samples on a hot stage on a polarizing microscope, by polarized light transmission intensity measurements and by wide angle X-ray diffraction analysis. The polymer from EtOVE, P(EtOVE), with a weight average molecular weight, $\bar{M}_w$, of less than about 8000 formed both smectic and nematic liquid crystalline, LC, phases after one heating cycle. In contrast, the polymer from this monomer which had an $\bar{M}_w$ of more than about 8000 exhibited only a nematic LC phase. For the polymer from HexOVE, P(HexOVE), both the narrow and broad MWD samples showed only a nematic LC phase over the $\bar{M}_w$ range from 2600 to 7300. The phase transitions of both types of polymers are discussed in relation to the molecular weight and MWD of the samples. The effect of the terminal group attached to the biphenyl group in the polymer is considered in relation to its possible steric effects.

(Keywords: molecular weight; phase transition; poly(vinyl ether); side-chain liquid crystal)

INTRODUCTION

Recently, the potential use of side chain liquid crystalline polymer, LCP, systems for application in electro-optical devices has received much attention[1–6], because of their combination of polymeric material properties and monomeric liquid crystalline properties. The main research activity on such side chain LCPs has been concentrated on their synthesis, on understanding their structure–property relations and on their electro-optical properties[7,8]. Although it is known that molecular weight (MW) and molecular weight distribution (MWD) are important factors which affect the thermal properties of the LCPs, there have been few studies on their effects so far. Our investigations have been concerned with this relationship for side-chain LCPs, and we have recently reported on the MW and MWD effects on the thermal properties of both narrow and broad MWD polymers. The polymers studied were obtained from 2-(4′-methoxy-4-biphenyloxy)ethyl vinyl ether[9] and from 2-(4′-cyano-4-biphenyloxy)ethyl vinyl ether[10], by using the living cationic polymerization reaction recently developed by Higashimura and coworkers (for reviews see References 11–14):

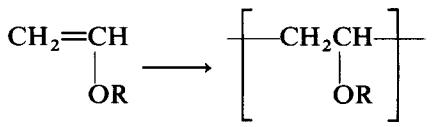

in which R represents the two different mesogenic groups.

Mesogen I, shown below, contained an electron donating methoxy group, while mesogen II, contained an electron withdrawing cyano group[9,10]:

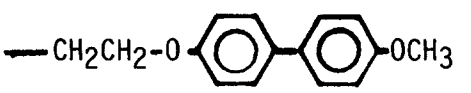

I

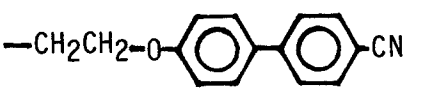

II

The relationships between the MW and MWD and the thermal properties of these polymers were complex. For the polymer with mesogen I at a given $\bar{M}_n$, a narrow MWD sample showed enantiotropic liquid crystalline behaviour and formed both smectic and nematic phases, but a broad MWD sample formed only a nematic phase. For the polymer with mesogen II, a low MW sample with a narrow MWD formed a smectic phase, but a high MW sample or a sample with a broad MWD exhibited only an amorphous character. These phenomena were interpreted on the basis of the relationship between the transition to or from the smectic phase and the glass transition temperature, T_g. That is, we concluded that these polymers had a monotropic smectic phase relative to the T_g.

In the present study polymers with mesogens III and IV

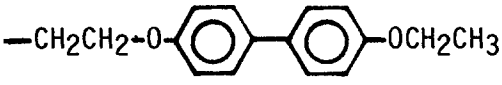

III

*Present address: Iwakuni Polymer Research Laboratory, Mitsui Petrochemical Industries Ltd, Waki-cho, Kuga-gun, Yamaguchi-ken, 740, Japan
† To whom correspondence should be addressed

0032-3861/89/122269-10$03.00

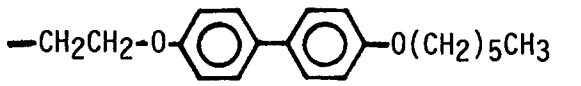

IV

having terminal alkoxy groups, either the ethoxy group or the hexyloxy group, both of which are larger in size than the previously studied methoxy group polymers, were prepared and characterized for their LC properties. The polymers were prepared by both traditional and living cationic polymerization reactions of the monomers 2-(4′-ethoxy-4-biphenyloxy)ethyl vinyl ether (EtOVE) and 2-(4′-hexyloxy-4-biphenyloxy)ethyl vinyl ether (HexOVE) shown below:

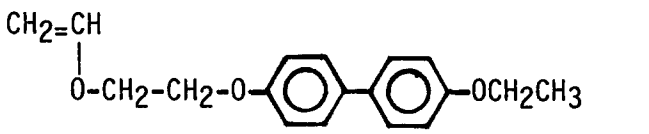

EtOVE

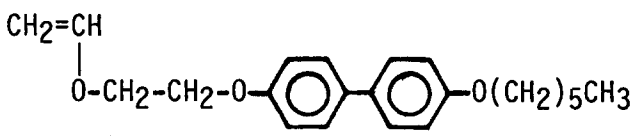

HexOVE

The phase transitions of the polymers were investigated in relation to their MW and MWD, and the effect of the terminal alkoxy group attached to the biphenyl group is considered in this paper.

EXPERIMENTAL

Monomers

2-(4′-Ethoxy-4-biphenyloxy)ethyl vinyl ether (EtOVE) and 2-(4′-hexyloxy-4-biphenyloxy)ethyl vinyl ether (HexOVE) were prepared by the phase transfer-catalysed condensation of 2-chloroethyl vinyl ether with the sodium salt of either 4-(4′-ethoxyphenyl)phenol or 4-(4′-hexyloxyphenyl)phenol, respectively, in the presence of a catalytic amount of tetrabutylammonium hydrogen sulphate (equation (2))[15]. The alkoxyphenylphenols were synthesized by the alkylation reactions of 4,4′-biphenol (equation (1))[15,16], as shown below:

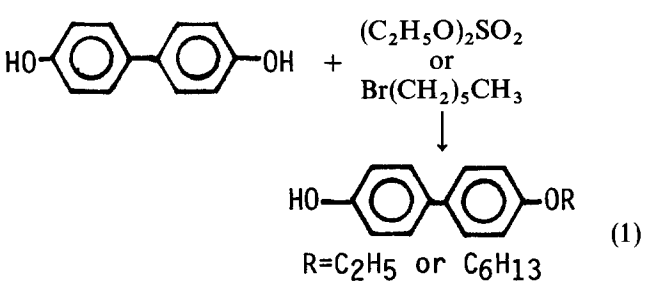

(1)

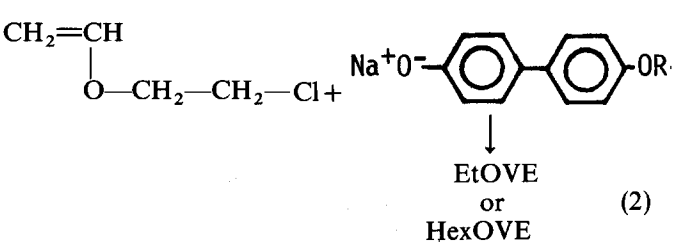

(2)

Table 1 Thermal properties[a] of the monomers

Monomer	T_m[b] (°C)	T_i[b] (°C)	T_d[c] (°C)	T_c[c] (°C)
EtOVE[d]	132	138	131	118
HexOVE	136	–	–	131

[a] Determined by d.s.c.
[b] Taken from the second heating cycle thermogram: T_m, melting temperature; T_i, isotropization temperature
[c] Taken from the first cooling cycle thermogram: T_d, deisotropization temperature; T_c, recrystallization temperature
[d] Enantiotropic liquid crystalline phase (smectic) was identified with the polarizing microscope

EtOVE and HexOVE were purified by recrystallization from methanol. Thermal transitions of the monomers as measured by differential scanning calorimetry (d.s.c.) and their ^{1}H- and ^{13}C-nuclear magnetic resonance (n.m.r.) chemical shifts are summarized in *Tables 1* and *2*.

Initiators and solvents

The hydrogen iodide (HI), iodine (I_2), zinc iodide (ZnI_2) and boron trifluoride etherate (BF_3OEt_2) initiators and the solvents (methylene chloride, n-hexane and diethyl ether) used were purified as previously reported[17–20].

Polymerization procedures

Cationic polymerization reactions were carried out in a dry-nitrogen atmosphere as previously reported[9,17–20]. All polymers were purified by precipitation from methylene chloride solution into methanol and dried in vacuum.

Fractionation and blending procedures

P(EtOVE) sample D (see *Table 3*), which was obtained by initiation with BF_3OEt_2, was not completely soluble in chloroform at room temperature after precipitation into methanol even though the polymer remained soluble until the end of the polymerization reaction in methylene chloride at −5°C. Therefore, sample D was separated into chloroform-soluble and -insoluble fractions by extraction with chloroform at room temperature at a concentration of 100 mg of polymer for 10 ml of solvent. The insoluble fraction, D–H, which represented 77 wt% of sample D, was recovered by filtration, and the soluble fraction, D–L, which represented the remainder was recovered by evaporation of the solvent. Both fractions were soluble in either *N*,*N*-dimethylformamide or nitrobenzene at an elevated temperature (60–80°C).

To prepare the blend of samples E and F (see *Table 4*), the two polymers were dissolved in *N*,*N*-dimethylformamide at 70°C. Concentrations of 100 mg/10 ml solvent were used for the preparation of blends of D–H, A and F. The blended polymers were recovered by precipitation from *N*,*N*-dimethylformamide solution into methanol and dried in vacuum before the characterization.

Characterization of monomers and polymers

The molecular weight distribution of the polymers was measured by gel permeation chromatography (g.p.c.) using $CHCl_3$ as the eluent on a Waters Associates Inc. liquid chromatograph equipped with five polystyrene gel columns (8 mm × 23 cm each) and a refractive index (RI)

Table 2 ^{1}H- and ^{13}C-n.m.r. chemical shifts[a] of the monomers and polymers

	EtOVE ($R = C^mH_2^mC^nH_3^n$)				HexOVE ($R = C^mH_2^mC^nH_2^nC^oH_2^oC^pH_2^pC^qH_2^qC^rH_3^r$)			
	^{1}H-n.m.r.		^{13}C-n.m.r.		^{1}H-n.m.r.		^{13}C-n.m.r.	
	δ (ppm)	Proton	δ (ppm)	Carbon	δ (ppm)	Proton	δ (ppm)	Carbon
Monomer	1.43(t)	n	15.7	n	0.90(t)	r	14.0	r
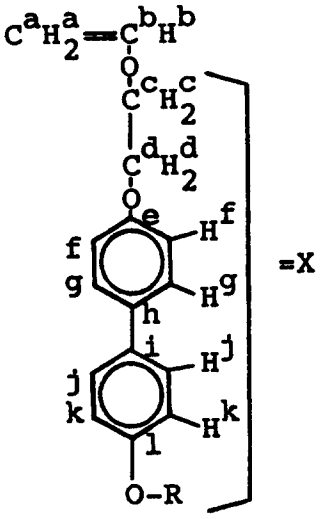	4.00–4.40(m)	a, c, d, m	64.3	m	1.00–1.90(m)	n, o, p, q, r	22.6	q
	6.50 (d of d)	b	67.1 and 67.3	c, d	3.80–4.30(m)	a, c, d, m	28.4	o
	6.75–7.05(m)	f, k	87.8	a	6.50 (d of d)	b	29.2	n
	7.40–7.55(m)	g, j	115.5 and 115.7	f, k	6.70–7.05(m)	f, k	31.6	p
			128.5	g, j	7.25–7.60(m)	g, j	66.3 and 66.4	c, d
			134.0 and 134.7	h, i			68.1	m
			152.4	b			87.0	a
			158.4 and 158.9	e, l			114.8 and 114.9	f, k
							127.7	g, j
							137.9	h, i
							151.8	b
							158.5 and 159.5	e, l
Polymer 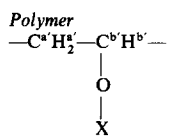	1.0–2.0	a′, n	40.6 and 41.7	a′	0.90	r	40.7 and 41.5	a′
	3.4–4.4	b′, c, d, m	74.5	b′	1.0–2.0	a′, n, o, p, q, r	73.9	b′
	6.7–7.1	f, k	c, d, . . ., n[b]		3.4–4.5	b′, c, d, m	c, d, . . ., r[b]	
	7.3–7.6	g, j			6.7–7.1	f, k		
					7.2–7.6	g, j		

[a] Chemical shifts are given in ppm relative to TMS
[b] The signals of the pendant groups (=X) are in the same position as those of the monomers

Table 3 Cationic polymerization of EtOVE and HexOVE[a]

Monomer	Polymer designation	Initiator (mM) solvent, temp. (°C)	$[M]_0$ (M)	Reaction time (h)	$10^{-3}M_n$ Calc.[b]	$10^{-3}M_n$ Obs.[c]	M_w/M_n[c]	DP_n[d]
EtOVE	A	HI/ZnI_2 (11.1/0.4), toluene, 40	0.09	24	2.3	2.0	1.1	7.0
	B	HI/I_2 (10.1/0.2), CH_2Cl_2, −5	0.10	24	2.8	2.6	1.1	9.2
	C	HI/ZnI_2 (3.1/0.2), CH_2Cl_2, −5	0.09	20	(5.3)[e]	–	(1.3)[e]	(18.7)[f]
	D	BF_3OEt_2 (2.5), CH_2Cl_2, −5	0.05	24	(4.0)[e]	–	(2.5)[e]	(14.1)[f]
	D–H[g]			(5.5)[e]	–		(2.2)[e]	(19.4)[f]
	D–L[h]				–	2.1	1.3	7.4
HexOVE	P	HI/ZnI_2 (5.7/0.3), CH_2Cl_2, −5	0.05	92	3.0	2.5	1.02	7.4
	Q	HI/ZnI_2 (10.1/0.4), toluene, 40	0.10	24	3.4	3.0	1.04	8.8
	R	BF_3OEt_2 (2.5), CH_2Cl_2, −5	0.05	24	–	2.8	2.6	8.2

[a] All reaction conversions were close to 100%, except sample C (=64%)
[b] M_n (calc.) = (MW of monomer) × ([M] consumed/$[HI]_0$)
[c] Determined by g.p.c. calibrated with standard polystyrene samples
[d] Number average degree of polymerization calculated from M_n (obs.)
[e] Hypothetical values (see text)
[f] Calculated from hypothetical M_n values
[g] $CHCl_3$ insoluble part of D = 77 wt%
[h] $CHCl_3$ soluble part of D = 23 wt%

detector. The number average and weight average molecular weights ($\bar{M}_n$ and $\bar{M}_w$) were calculated with the use of a standard polystyrene calibration curve.

^{1}H (200 or 300 MHz) and ^{13}C (75.4 MHz) n.m.r.spectra were obtained with Varian XL-200 or XL-300 spectrometers in $CDCl_3$ at room temperature. The chemical shifts of the ^{1}H- and ^{13}C-n.m.r. spectra of the monomers (EtOVE and HexOVE) and the corresponding polymers are summarized in *Table 2*. As the chemical shifts of the monomers and their polymers indicate, after the polymer-

Table 4 Thermal properties of poly(EtOVE)s

Polymer designation	$10^{-3}\bar{M}_w/10^{-3}\bar{M}_n/\bar{M}_w/\bar{M}_n$	Thermal transitions (°C) by d.s.c.						Thermodynamic parameters[c]			
		Heating cycle[a]			Cooling cycle[b]			ΔH (cal g^{-1})		$10^2\Delta S$ (cal g^{-1} K^{-1})	
		T_g	T_{s-n}	T_{n-i}	T_{i-n}	T_{n-s}	T_g	ΔH_{s-n}	ΔH_{n-i}	ΔS_{s-n}	ΔS_{n-i}
A	2.2/2.0/1.1	122 (141)	– (177)	175 (182)	176	160	120	9.4	2.2	2.1	0.5
D–L[d]	2.7/2.1/1.3	127 (144)	– (178)	178 (185)	175	158	125	9.0	2.2	2.0	0.5
B	2.9/2.6/1.1	141 (147)	– (175)	181 (183)	170	152	123	9.4	3.1	2.1	0.7
E[e]	(4.4/2.3/1.9)[f]	147 (145)	– (173)	199 (193)	167	147	125	7.1	6.0	1.6	1.3
C	(6.9/5.3/1.3)[f]	173 (162)	– (176)	194 (187)	168	153	139	5.8	6.1	1.3	1.3
F[e]	(8.8/3.5/2.5)[f]	195 –[g]	– –	206 (189)	176	–	–[g]	–	13.0	–	2.8
D	(10.0/4.0/2.5)[f]	195 –[g]	– –	209 (212)	191	–	–[g]	–	13.1	–	2.7
D–H[d]	(12.1/5.5/2.2)[f]	202 –[g]	– –	210 (211)	191	–	–[g]	–	15.2	–	3.1

[a] Taken from the first heating cycle; numbers in parentheses indicate the transition temperatures taken from the second heating cycle
[b] Taken from the first cooling cycle
[c] Taken from the second heating cycle
[d] High and low MW portions of sample D by fractionation (see text)
[e] Blend polymers of samples D–H and A; E = 22/78, F = 67/33 wt% (see text)
[f] Hypothetical values (see text)
[g] T_g may overlap with T_{n-i} or T_{i-n}

ization the signals of the vinyloxy group in the monomers (^{1}H-n.m.r., 6.50 ppm for both EtOVE and HexOVE (CH_2=C<u>H</u>–O–); ^{13}C-n.m.r., 87.8 (C^a) and 152.4 ppm (C^b) for EtOVE, 87.0 (C^a) and 151.8 ppm (C^b) for HexOVE ($\underline{C}^aH_2$=$\underline{C}^bH$–O–) disappeared and new signals corresponding to the main chain methylene and methine structure (^{1}H-n.m.r., 1.0–2.0 and 3.4–4.3 ppm (–CH_2–C<u>H</u>–); ^{13}C-n.m.r., 40.6 and 41.7 ppm for EtOVE and 73.9 ppm for HexOVE (–CH_2–$\underline{C}$H–)) appeared. Both ^{1}H- and ^{13}C-n.m.r. spectra also showed that the signals of the pendant group (X in *Table 2*) are exactly the same as those of the monomers with some peak broadening.

Thermal analyses were carried out on a Perkin–Elmer DSC-2 instrument with polymer and monomer samples of 5–10 mg under a nitrogen flow at a scanning rate of 10°C min^{-1}. Indium and naphthalene were used for the calibration of the temperature scale. The melt behaviour of the polymers was visually observed using a polarizing light microscope equipped with cross-polarizers and a hot stage.

The apparatus used for light transmission studies contained a laser, a polarizer, a Mettler hot stage and a photomultiplier. A Spectra Physics He–Ne gas laser (λ = 6358 Å*) was used as a light source.

X-ray diffraction experiments were carried out on a Statton flat film camera using Ni-filtered CuKα radiation (λ = 1.542 Å) under reduced pressure. The powder samples were sealed in glass capillaries, and a home-made hot stage was used to control the sample temperature within 1°C.

RESULTS AND DISCUSSION

Polymerization of EtOVE and HexOVE

The cationic polymerization of EtOVE or HexOVE was carried out with the HI/I_2 and the HI/ZnI_2 initiators, both of which are reported to be living-polymerization initiator systems[11–14,17–19], and also with boron trifluoride etherate (BF_3OEt_2), which is a conventional cationic initiator. The polymerization conditions and the MW values of the polymers so obtained are summarized in *Table 3*. *Figures 1* and *2* show the MWDs of the polymers.

Polymers A, B, P, Q and R were soluble in the polymerization solvent at the polymerization temperatures and in the $CHCl_3$ at room temperature for the g.p.c. measurements. All polymers had the expected structures, as indicated by the n.m.r. data in *Table 2*. As previously reported[9,10], the HI/I_2- or HI/ZnI_2-initiated reactions gave polymers (polymers A, B, P and Q) with narrow MWDs and with $\bar{M}_w/\bar{M}_n$ ratios varying from 1.02 to 1.1. In contrast, the BF_3OEt_2-initiated polymers had a broad

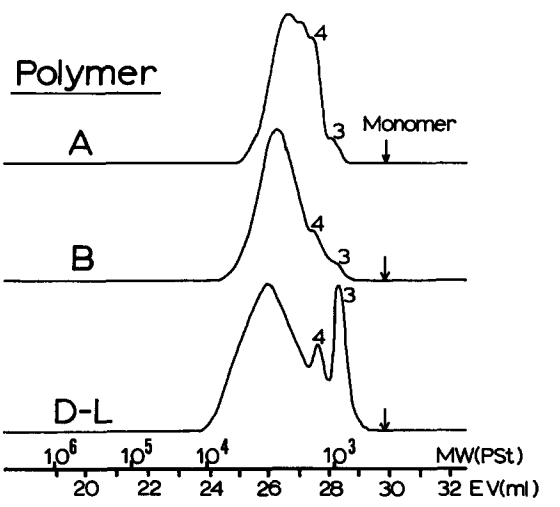

Figure 1 MWD of P(EtOVE); see *Table 3* for reaction conditions. Numbers near the peaks indicate the degree of polymerization of the sample

* 1 Å = 10^{-1} nm

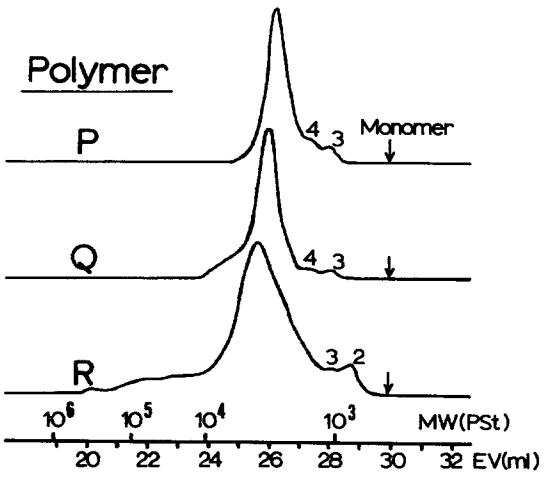

Figure 2 MWD of P(HexOVE); see *Table 3* for reaction conditions. Numbers near the peaks indicate the degree of polymerization of the sample

MWD, as shown in *Table 3* and *Figures 1* and *2*. The MWs and the solubility of polymers C and D are described in the Experimental section above.

Phase transitions of the EtOVE polymers P(EtOVE)

Typical thermograms obtained for the HI/ZnI_2 polymers and for the BF_3OEt_2 polymers are shown in *Figures 3* and *4*, respectively. Polymer A, having a low MW and a narrow MWD showed a glass transition, T_g, at 122°C and an endothermic peak, T_1, at 175°C in the first heating cycle (see *Figure 3*), and exothermic peaks, T_2 at 176°C and T_3 at 160°C, and a T_g at 120°C in the first cooling cycle. A T_g at 141°C and endothermic peaks, T_4 at 177°C and T_5 at 182°C, in the second heating cycle were also observed.

In contrast, as shown in *Figure 4*, polymer D, with a relatively high MW and with a broad MWD, exhibited a T_g at 195°C and an endothermic peak, T_1, at 209°C, in the first heating cycle, an exothermic peak, T_2, at 191°C, in the first cooling cycle, and an endothermic peak, T_5, at 212°C in the second heating cycle. After the first heating cycle, subsequent cycles for both polymer A and polymer D gave virtually identical d.s.c. thermograms.

To identify the phases present before and after the transition peaks T_1–T_5, texture observations were made with a polarized light microscope. For polymer A, nematic threaded textures[21] (see *Figure 5a*) were observed at temperatures below T_1 in the first heating cycle, between T_2 and T_3 in the first cooling cycle, and between T_4 and T_5 in the second heating cycle. The nematic threaded texture did not change even after the sample was kept below T_2 (173°C) for 30 min in the first cooling cycle. A smectic fan-shaped texture[21] (see *Figure 5b*) was observed below T_3 in the first cooling cycle and below T_4 in the second heating cycle. The same phase transition phenomena were observed for polymers D–L, B, E and C.

In contrast, polymers D, F and D–H exhibited nematic threaded textures[21] (*Figure 5c*) at temperatures below T_1, T_2 and T_5 (see *Figure 4*). The nematic texture did not change when polymer D was kept just below T_2 (188°C) for 30 min in the first cooling cycle.

Each transition peak and each phase before and after the peak could be identified in this manner, and the transitions are represented in *Figure 6*, in which T_{x-y} indicates the transition temperature from the x-phase to the y-phase. The assigned transitions are also listed in *Table 4*, and the transition temperatures of P(EtOVE) as a function of $\bar{M}_w$ are shown in *Figure 7*.

From the data in *Table 4* and *Figure 7*, three conclusions can be drawn for this polymer:

(1) With increasing MW, the T_g and T_{n-i} increased, but T_{s-n} was not affected. As a result, the temperature range above T_g and below T_{g-n} for the smectic LC phase became increasingly narrow and, at an $\bar{M}_w$ of approximately 8000, the smectic phase did not appear.

(2) At approximately the same $\bar{M}_n$, the broad distribution sample, F, had different thermal properties, including a higher T_g and T_{n-i} but no T_{s-n}, from those of the narrow distribution sample, B. Possibly, the T_g and T_{n-i} values were strongly affected by the higher MW fraction of the broad distribution polymer.

(3) Polymers F, D and D–H, for which the virgin polymers were recovered by precipitation into methanol, showed T_g transitions only in the first heating cycle, and they did not show clearly a T_g after one heating cycle. In some cases the T_g overlapped with the T_{i-n} or T_{n-i} transitions after one heating cycle in the same manner as previously reported for the polymers from 2-(4′-

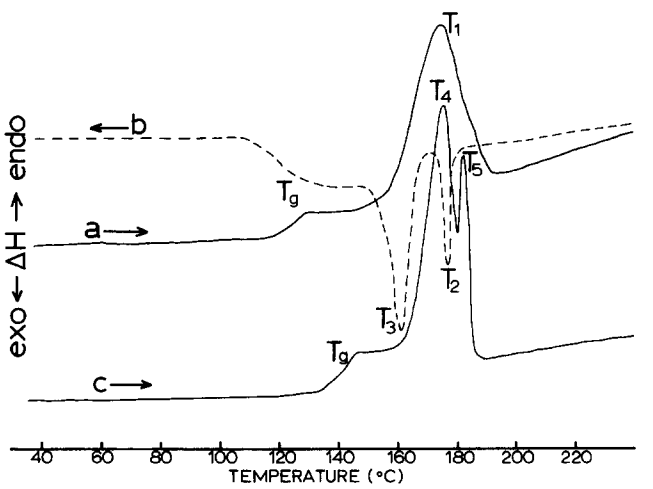

Figure 3 D.s.c. thermograms of P(EtOVE), polymer A, obtained by initiation with HI/ZnI_2: (a) first heating cycle, (b) first cooling cycle, (c) second heating cycle

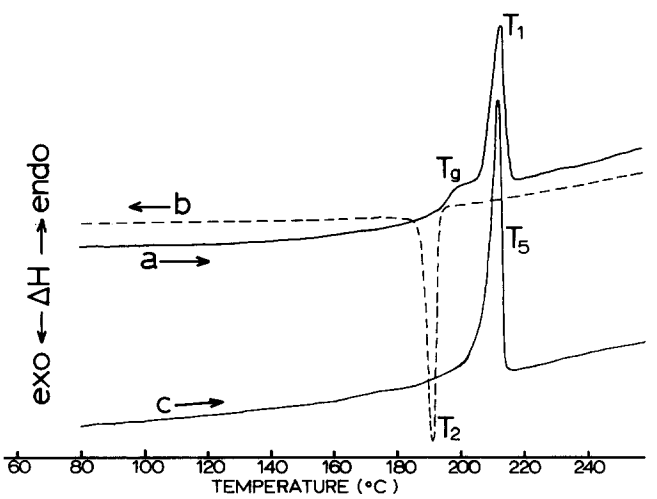

Figure 4 D.s.c. thermograms of P(EtOVE), polymer D, obtained by initiation with BF_3OEt_2: (a) first heating cycle, (b) first cooling cycle, (c) second heating cycle

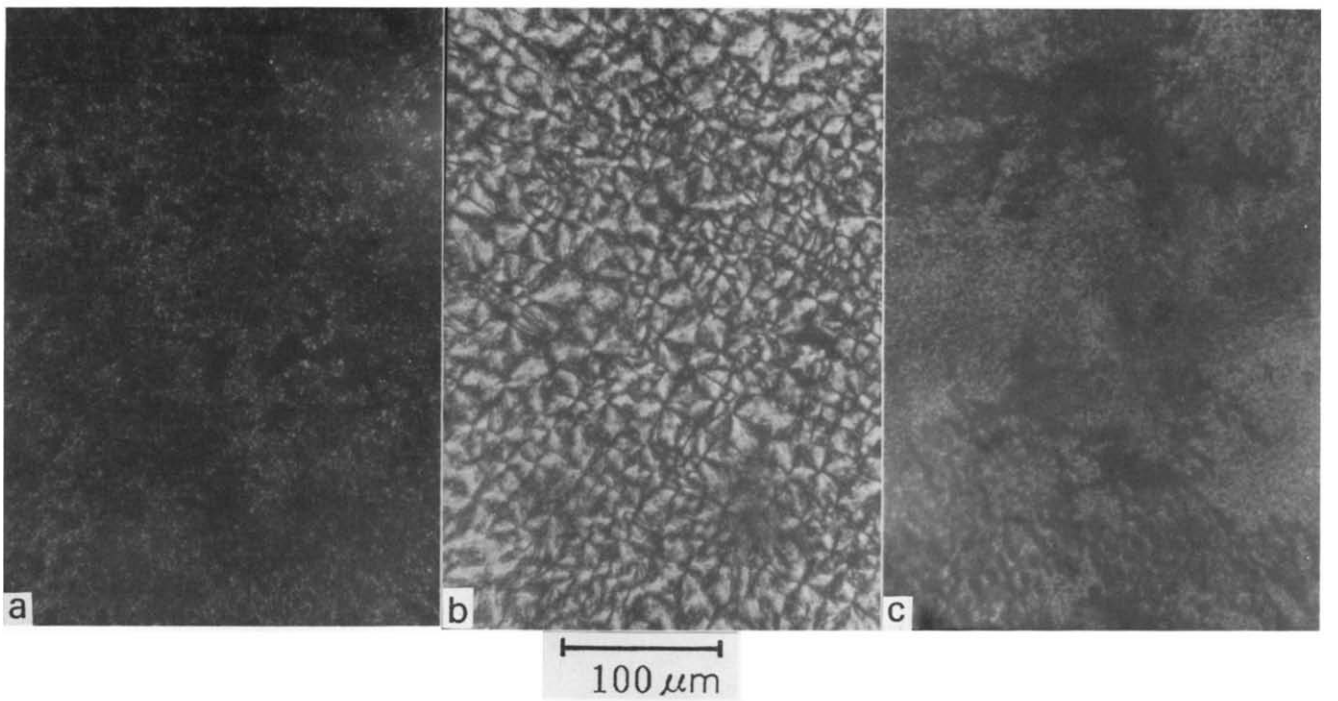

Figure 5 Photomicrographs of P(EtOVE) showing: (a) nematic threaded texture of polymer A at 173°C (between T_2 and T_3); (b) smectic fan-shaped texture of polymer A at 150°C (below T_3); (c) nematic threaded texture of polymer D at 188°C (below T_2); all photographs were taken during the first cooling cycle (magnification: 320)

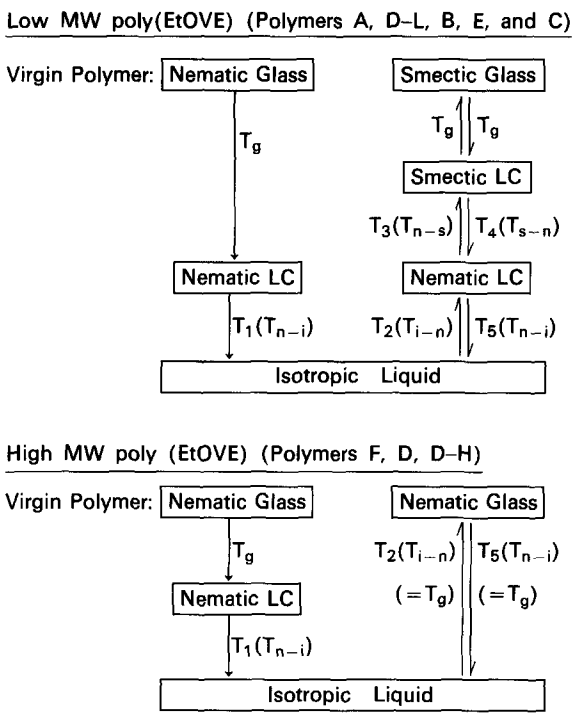

Figure 6 Schematic representation of the comparative thermal transitions of low and high MW samples of P(EtOVE)

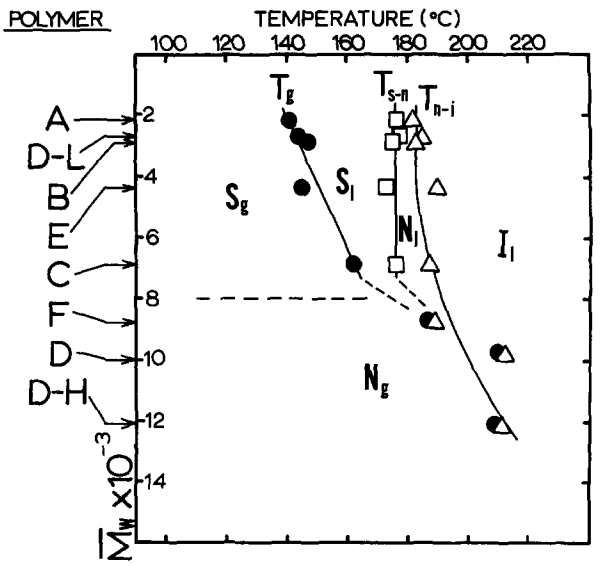

Figure 7 Phase diagram of P(EtOVE) as a function of $\bar{M}_w$, showing transition temperatures during the second heating cycle of the d.s.c. thermograms: I, isotropic; N, nematic; S, smectic,; l, liquid; g, glass

methoxy-4-biphenyloxy)ethyl vinyl ether[9] and 2-(4'-cyano-4-biphenyloxy)ethyl vinyl ether[10].

The MW effects on the phase transitions of this polymer can be summarized as follows: during the cooling cycle, the higher MW polymers, most likely those with an $\bar{M}_w > 8000$, form a glass phase and become immobile before they can reorganize from the nematic to a smectic phase, so the transition only from the isotropic to the nematic phase occurs. In contrast, when MW is low, the T_g is low too, and the sample can form a smectic phase from the nematic phase before the T_g is reached during the cooling cycle. That is, the former polymer apparently also has a monotropic smectic phase relative to T_g in the same manner as the polymers previously reported[9,10].

Transmitted light intensity and X-ray diffraction analyses of P(EtOVE)

To confirm the phase transition behaviour of P(EtOVE) observed by d.s.c. and by use of a polarizing light microscope, two additional measurements were made: first, transmitted light intensity and, second, wide angle

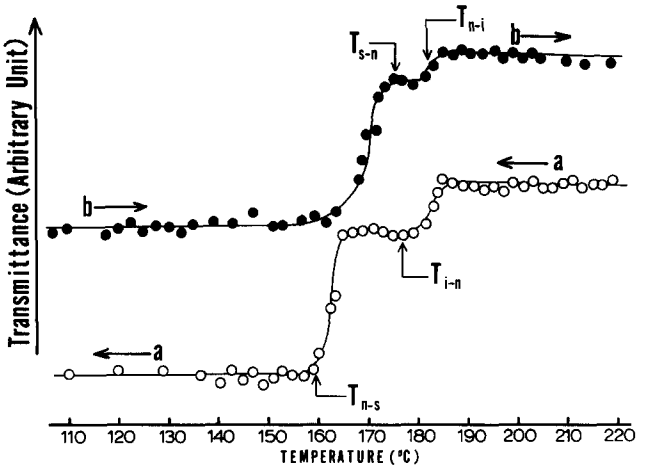

Figure 8 Transmitted light intensity as a function of sample temperature for (a) the first cooling cycle and (b) the second heating cycle of P(EtOVE), polymer A, obtained by initiation with HI/ZnI_2

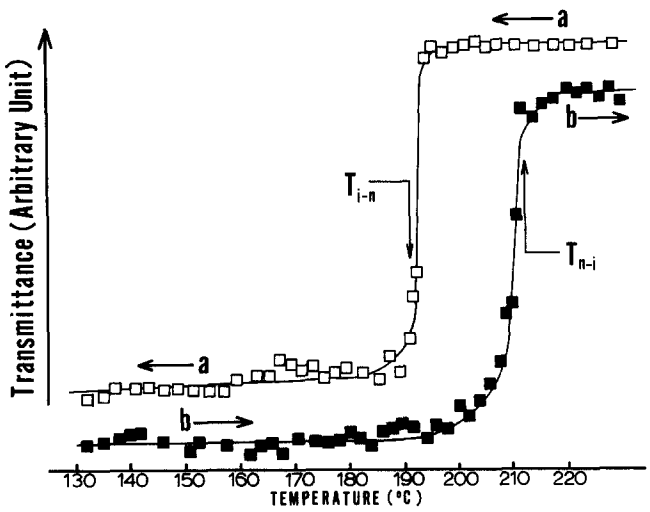

Figure 9 Transmitted light intensity as a function of sample temperature for (a) the first cooling cycle and (b) the second heating cycle of P(EtOVE), polymer D, obtained by initiation with BF_3OEt_2

X-ray diffraction (WAXS). *Figures 8* and *9* show the transmitted light intensity of polymers A and D, respectively, as a function of sample temperatures in the first cooling cycle and in the second heating cycle. For polymer A in *Figure 8*, two changes in intensity can be seen during both the first cooling cycle and the second heating cycle. These changes correspond closely to T_{i-n} and T_{n-s} in the first cooling cycle and to T_{s-n} and T_{n-i} in the second heating cycle as measured by d.s.c. (see *Figure 3*). For polymer D in *Figure 9*, only one change of the transmitted light intensity is seen in each scan, and this change also corresponds to either T_{i-n} or T_{n-i} as determined by d.s.c. (see *Figure 4*).

Table 5 shows the WAXD data for polymer A in the nematic phase and in the smectic phase and for polymer D–H in the nematic phase. Both the nematic and the smectic phase show diffuse rings at wide angles for the intermolecular spacing perpendicular to the mesogen long axes of the side-chains. The average intermolecular spacings observed of 4.19–4.34 Å are consistent with those reported for this type of side-chain LCP[22,23].

At smaller diffraction angles, the WAXD patterns of the nematic and the smectic phase were different. The patterns of the smectic phase are characterized by a sharp, intense ring with both medium strength and second-order and weak third-order reflections corresponding to a layer thickness of 29.0 Å. This value is considerably greater than the length of the side-chain, 19–20 Å, in its fully extended conformation. Thus, the existence of some form of bilayer structure in the smectic phase, in which the molecules partially overlap, appears to be verified, as previously reported for the polymer from a cyanobiphenyl-containing acrylate monomer[23].

For the nematic phase, diffuse rings which correspond to a distance of 12.8–13.3 Å were observed. This value is approximately the length of 4,4'-diethoxybiphenyl, so it may arise from the intramolecular spacings parallel to the long axes of the side-chain in the same manner as some nematic main-chain LCP show a diffuse ring corresponding to distances close to, or equal to, the repeating unit length[24]. This result is an indication that there is no order in the direction of the molecular long axes.

In conclusion, the transmitted light intensity and X-ray diffraction data confirm that the low MW samples of P(EtOVE) had different phase transition behaviour from that of high MW samples, as summarized in *Figure 6*.

Phase transitions of the HexOVE polymers, P(HexOVE)

The d.s.c. thermograms of the polymer obtained by HI/ZnI_2 initiation, P in *Table 3*, and by BF_3OEt_2 initiation, R in *Table 3*, in the polymerization of HexOVE are shown in *Figure 10*. Photomicrographs of polymers P and R, both of which exhibit nematic threaded textures[21], are shown in *Figure 11*. The nematic textures did not change after the samples were kept below T_{i-n} for 30 min in the first cooling cycle. From these data, it may be concluded that polymers P, Q and R all form only a nematic LC phase between T_g and the isotropization temperature, T_{n-i}, in the moleculr weight $2600 \leqslant \bar{M}_w \leqslant 7300$. The thermal properties of these polymers are summarized in *Table 6*.

With increasing MW, the T_g of P(HexOVE) increased as expected, but unexpectedly T_{n-i} and T_{i-n} decreased, as shown in *Table 6*. As a result, the temperature range of the nematic LC phase between T_g and T_{n-i} or T_{i-n} became narrower with increasing MW. For example, polymer R, which had approximately the same $\bar{M}_n$ as that of polymer P but had a broader MWD, showed a

Table 5 X-ray diffraction analysis data of poly(EtOVE)s: interplanar *d* spacings of polymers A and D–H[a–c]

	Polymer A		Polymer D–H
	At 170°C (nematic)	At 135°C (smectic)	at 185°C (nematic)
Small angles			
$d_1 \pm 1$ (Å)	–	29.0(S)	–
$d_2 \pm 0.2$ (Å)	12.8(W)	14.5(M)	13.3(W)
$d_3 \pm 0.2$ (Å)	–	9.74(W)	–
Wide angles			
$d_4 \pm 0.04$ (Å)	4.29(M)[d]	4.34(M)[e]	4.19(M)[f]

[a] Measured in the first cooling cycle after the samples melted to isotropic liquid
[b] Numbers are taken from diffraction maxima
[c] Intensities of the diffractions are given in parentheses as: S, strong; M, medium; W, weak
[d–f] Diffuse diffraction rings with *d* values 3.9–5.1, 3.9–4.9, 3.9–4.9 Å, respectively

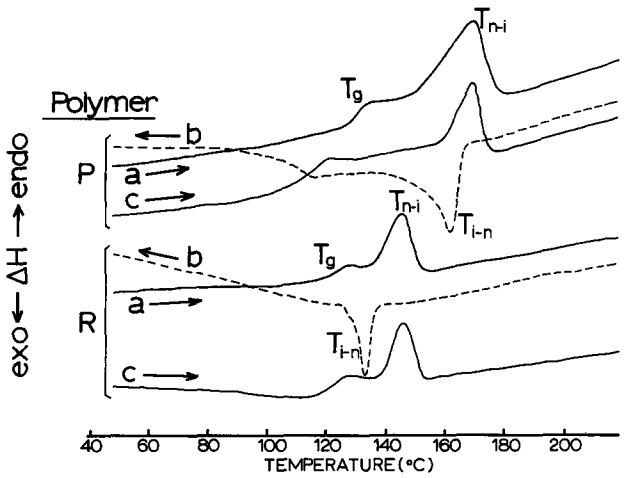

Figure 10 D.s.c. thermograms of P(HexOVE) obtained by initiation with HI/ZnI_2, polymer P, and with BF_3OEt_2, polymer R: (a) first heating cycle; (b) first cooling cycle; (c) second heating cycle

much narrower temperature range for its nematic LC phase. It appears likely, therefore, that the thermal transitions of this polymer were more strongly affected by the higher molecular weight fraction in the broad distribution sample, in the same manner as we previously reported for other LC poly(vinyl ether)s[9,10].

Effect of terminal substituent in the biphenyl group

To obtain a semi-quantitative indication of the steric effect of the terminal substituents, the bulkiness factor of the substituent, R, attached to the biphenyl group is calculated by the following equation:

$$\text{bulkiness factor (A)} = \sum (\text{bond length} + \text{van der Waals radius of the end atom})$$

The bulkiness factor is the distance from the centre of the carbon atom at the 4′-position of the biphenyl group to the end of the substituent and is calculated by assuming that the substituent is fully extended. The bulkiness

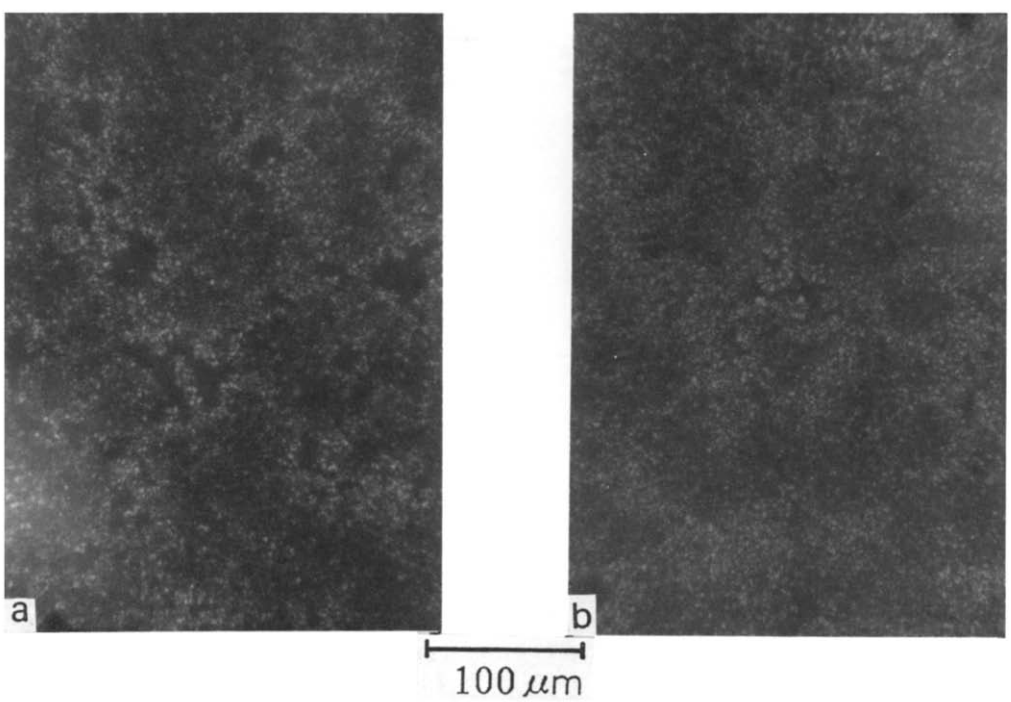

Figure 11 Photomicrographs of the nematic threaded textures of samples of P(HexOVE): (a) polymer P at 155°C (just below T_{i-n}) in the first cooling cycle; (b) polymer R at 125°C (just below T_{i-n}) in the first cooling (magnification: 320)

Table 6 Thermal properties of poly(HexOVE)s

Polymer designation	$10^{-3}\bar{M}_w/10^{-3}\bar{M}_n/\bar{M}_w/\bar{M}_n$	Thermal transitions (°C) by d.s.c.				Thermodynamic parameters[c]	
		Heating cycle[a]		Cooling cycle[b]		ΔH_{n-i}	ΔS_{n-i}
		T_g	T_{n-i}	T_{i-n}	T_g	(cal g^{-1})	(cal g^{-1} K^{-1})
P	2.6/2.5/1.02	126 (106)	168 (169)	161	105	8.3	1.9
Q	3.1/3.0/1.04	131 (111)	171 (156)	144	108	9.9	2.3
R	7.3/2.8/2.6	127 (120)	148 (148)	135	–[d]	4.8	1.1

[a] Taken from the first heating cycle; numbers in parentheses indicate the transition temperatures taken from the second heating cycle
[b] Taken from the first cooling cycle
[c] Taken from the second heating cycle
[d] T_g may overlap with T_{i-n}

factors so calculated and the abbreviation for each monomer unit are as follows:

R=H: 2.3 Å; HVE
R=CN: 4.2 Å; CNVE
R=OMe: 5.1 Å; MeOVE
R=OEt: 6.6 Å; EtOVE
R=OHex: 12.8 Å; HexOVE

Figure 12 shows the general phase diagram for the polymers in this series having different terminal substituents as a function of the bulkiness factor of the substituents. The data in *Figure 12* are only for the polymers with narrow MWDs ($\bar{M}_w/\bar{M}_n \leqslant 1.3$) and with $\bar{M}_n$ from 2000 to 2500. PHVE did not show a mesophase, but all of the other polymers in the series above exhibited at least one mesophase. With increasing bulkiness factor, the isotropization temperatures of the polymers, from either the nematic or the smectic phase, increased from R=CN to R=OEt but did not increase from R=OEt to R=OHex, while the T_g increased from R=H to R=OMe but decreased from R=OMe to R=OHex. As a result, the temperature range of the LC phase became wider with increasing bulkiness factor.

Inspection of *Figure 12* also reveals that each of the LC polymers exhibited different types of mesophase transitions which may be related to the different lengths of the terminal substituents. The transitions observed for each were as follows:

P(HVE), amorphous glass to isotropic liquid;
P(CNVE), smectic glass to isotropic liquid;
P(MeOVE), smectic glass to nematic liquid to isotropic liquid;
P(EtOVE), smectic glass to smectic liquid to nematic liquid to isotropic liquid;
P(HexOVE), nematic glass to nematic liquid to isotropic liquid.

To explain these observations we can classify the substituents according to their size (small, medium, and large) and polarity as shown in *Figure 13*. For example, for P(CNVE) the CN substituent is not only small but it is also highly polar, and the enhanced interaction between mesogens may aid in formation of the smectic phase instead of a nematic phase. On the other hand, for the polymers with less polar alkoxy terminal group, there may be an optimum size of R to form a smectic phase.

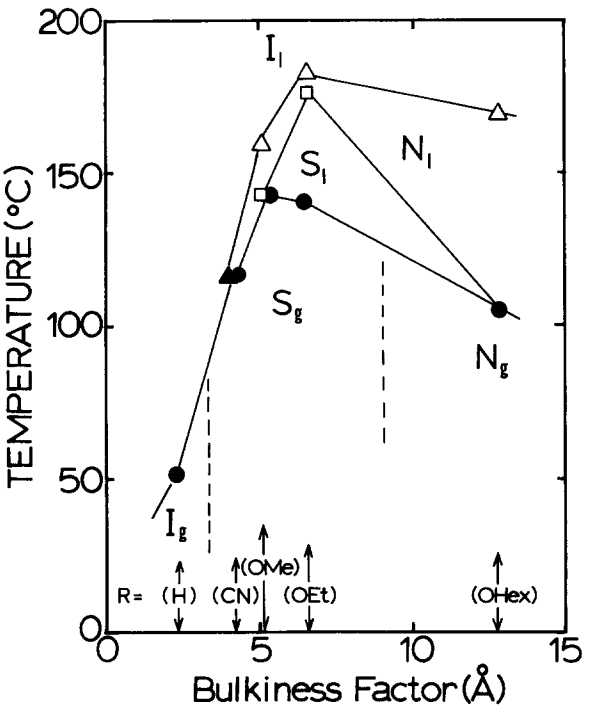

Figure 12 Phase diagram of the poly(vinyl ether)s of this series with various terminal substituents as a function of the bulkiness factor of R. Transition temperatures are those in the second heating cycle: ●, T_g; ▲, T_{s-i}; □, T_{s-n}; △, T_{n-i}. I, isotropic; N, nematic; S, smectic; l, liquid; g, glass

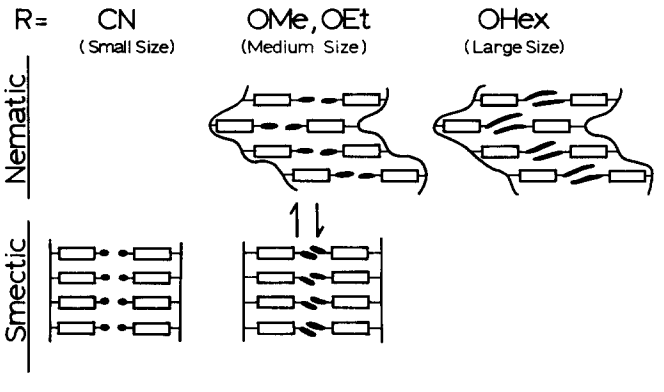

Figure 13 Schematic representation of the relationship between size of the terminal substituent and type of mesophase

ACKNOWLEDGEMENTS

The authors are grateful to the National Science Foundation for the support of this work and Mitsui Petrochemical Industries Ltd for the support of Toshihiro Sagane. We are grateful to Dr S. K. Bhattacharya for the transmitted light intensity analysis and to Mr J. J. Mallon of the Polymer Science and Engineering Department for X-ray diffraction analysis.

REFERENCES

1 Krigbaum, W. R. and Lader, H. J. *Mol. Cryst. Liq. Cryst.* 1980, **62**, 87
2 Finkelmann, H. and Ringsdorf, H. *Makromol. Chem.* 1978, **179**, 273
3 Ringsdorf, H. and Schneller, A. *Br. Polym. J.* 1981, **13**, 43
4 Ringsdorf, H. and Zentel, R. *Makromol. Chem.* 1978, **180**, 803
5 Finkelmann, H., Keichle, U. and Rehage, G. *Mol. Cryst. Liq. Cryst.* 1983, **94**, 343
6 Coles, H. J. and Simon, R. in 'Recent Advances in Liquid Crystalline Polymers' (Ed. L. L. Chapoy), Elsevier Applied Science, New York, 1985, Ch. 22
7 Finkelmann, H. and Rehage, G. *Adv. Polym. Sci.* 1984, **60/61**, 99
8 Shibaev, V. P. and Plate, N. A. *Adv. Polym. Sci.* 1984, **60/61**, 173
9 Sagane, T. and Lenz, R. W. *Polym. J.* 1988, **20**, 923
10 Sagane, T. and Lenz, R. W. *Macromolecules* in press
11 Higashimura, T. and Sawamoto, M. *Adv. Polym. Sci.* 1984, **62**, 49
12 Higashimura, T. and Sawamoto, M. *Macromol. Chem. Suppl.* 1985, **12**, 153
13 Sawamoto, M. and Higashimura, T. *Makromol. Chem. Makromol. Symp.* 1986, **3**, 83
14 Higashimura, T., Aoshima, S. and Sawamoto, M. *Makromol. Chem. Makromol. Symp.* 1986, **3**, 99
15 Rodriguez-Parada, J. M. and Percec, V. *J. Polym. Sci., Polym. Chem. Edn.* 1986, **24**, 1363

16 Gray, G. W., Harrison, K. J., Nash, J. A., Constant, J., Hulme, D. S., Kirton, J. and Raynes, E. P. in 'Liquid Crystals and Ordered Fluids', Vol. 2 (Eds J. F. Johnson and R. S. Porter), Plenum Press, New York, 1974, p. 617
17 Miyamoto, M., Sawamoto, M. and Higashimura, T. *Macromolecules* 1984, **17**, 265
18 Miyamoto, M., Sawamoto, M. and Higashimura, T. *Macromolecules* 1984, **17**, 2228
19 Enoki, T., Sawamoto, M. and Higashimura, T. J. *J. Polym. Sci., Polym. Chem. Edn.* 1986, **24**, 2261
20 Sawamoto, M., Okamoto, C. and Higashimura, T. *Macromolecules* 1987, **20**, 2693
21 Demus, D. and Richter, L. 'Textures of Liquid Crystals', Verlag Chemie, New York, 1978
22 Tsukruk, V. V., Shilov, V. V., Konstantinov, I. I., Lipatov, Yu. S. and Amerik, Yu. B. *Eur. Polym. J.* 1982, **18**, 1015
23 Barny, P. L., Dubois, J.-C., Friedrich, C. and Noel, C. *Polym. Bull.* 1986, **15**, 341
24 Noel, C. in 'Recent Advances in Liquid Crystalline Polymers' (Ed. L. L. Chapoy), Elsevier Applied Science, New York, 1985, Ch. 9